UVCS/SOHO Observations of Jupiter in January 1997: An Independent Calibration of the White Light Channel

Steven R. Cranmer
Harvard-Smithsonian Center for Astrophysics, 60 Garden Street, Cambridge, MA 02138
14 July 1999 (original version), 27 June 2001 (revised version)

1. Introduction

On 16 January 1997, UVCS/SOHO observed the planet Jupiter, which was reaching its quasi-yearly opposition with the vector between the Earth and the Sun. In this set of notes we predict Jupiter's white light emission for that time period and compare the predicted emission with the observed count rates. The goal of this study was to refine the absolute photometric calibration for the UVCS White Light Channel (WLC). It should be noted that in June 2001, UVCS/SOHO observed Jupiter again with a much more systematic observing plan, and the results of that more careful study should supersede those herein.

2. Predicted Intensities

At visible wavelengths, Jupiter reflects the light of the Sun and does not emit any radiation of its own (this is not the case in the infrared and radio). Thus, we can use a solar spectrum, convolved with the *albedo*, or reflecting efficiency, of Jupiter, to derive its expected brightness in the sky.

Figure 1 shows a sampling of the "coarse" solar flux atlas of Kurucz et al. (1984), which has a wavelength resolution of 0.2–0.4 Å and contains thousands of absorption lines. This is the flux per unit wavelength at the orbit of the Earth, $F_{\lambda\oplus}$, in units of photons s^{-1} cm^{-2} $Å^{-1}$.

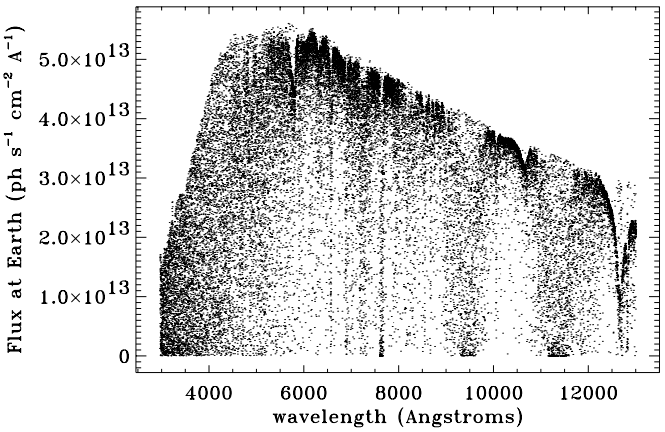

Figure 1: *Solar flux at 1 AU.*

From this data we can compute two quantities that will be useful later. First, the disk-center surface brightness of the Sun, $B_{\lambda\odot}$, familiar as the normalization for quoted pB measurements, is given by

$$B_{\lambda\odot} \;=\; \frac{5}{4\pi} F_{\lambda\oplus} \left(\frac{r_{1\mathrm{AU}}}{R_\odot}\right)^2 \;\approx\; 18383\, F_{\lambda\oplus} \tag{1}$$

where the inverse-square decrease in the flux from the Sun to the Earth is accounted for, and the outgoing flux is converted into a disk-center specific intensity by multiplying by $5/4\pi$ (this factor comes from a gray atmosphere computed using the Eddington approximation).

Second, the solar flux incident on Jupiter's surface is given by

$$F_{\lambda\mathrm{J}} \;=\; F_{\lambda\oplus} \left(\frac{r_{1\mathrm{AU}}}{r_{\odot\mathrm{J}}}\right)^2 \;. \tag{2}$$

The 1997 *Astronomical Almanac* gives a Sun-Jupiter distance of $r_{\odot\mathrm{J}}$ = 5.1320 AU for 16 January 1997 (interpolation from tabular data was required).

The disk-center specific intensity *reflected* by Jupiter is given by the product of its wavelength-dependent albedo and the incident solar intensity:

$$I_{\lambda\mathrm{J}} \;=\; \frac{5}{4\pi}\, F_{\lambda\mathrm{J}}\, a_\lambda \tag{3}$$

and the geometric albedo a_λ (defined precisely as the ratio of the planet's radiance to the radiance of a perfect diffuser of the same size) is given by Harris (1961) for the U, B, V, R, and I photometric bands:

Jovian Geometric Albedo

Band	$\lambda_{\mathrm{central}}$ (Å)	a_λ
U	3600	0.270
B	4500	0.370
V	5600	0.445
R	6750	0.466
I	8000	0.347

The estimated uncertainty in these values is approximately $\pm$ 5%, and we linearly interpolate between these points to compute a_λ as a continuous function of wavelength. Ideally, there should be sharp line-like features in the albedo, arising from the fact that atoms and molecules in Jupiter's atmosphere absorb radiation differently from the solar atmosphere. The strongest Jovian absorption features are known to be in the infrared (see, e.g., Drossart & Encrenaz 1983), but an actual spectrum of Jupiter should be consulted to make sure these effects are not large in the visible.

3. WLC Instrumental Effects

The UVCS WLC collects photons in a specific bandpass between 4000 and 6000 Å. The bandpass transmittance is the product of two components: T_1, from the spectral response of the color filter, and T_2, from the wavelength-dependent sensitivity of the photomultiplier tube. Benchmark measurements of both T_1 and T_2 were made by the UVCS team during its end-to-end test, and the results have been provided by

Fineschi (1999, private communication). Figure 2 shows the product of T_1 and T_2, linearly interpolated onto a constant wavelength grid. (Note that T_1 has a finer, quasi-sinusoidal structure on a $\sim$10 Å scale, but these features average out on the larger scale.) We estimate the uncertainty in this function to be no more than $\pm$5%.

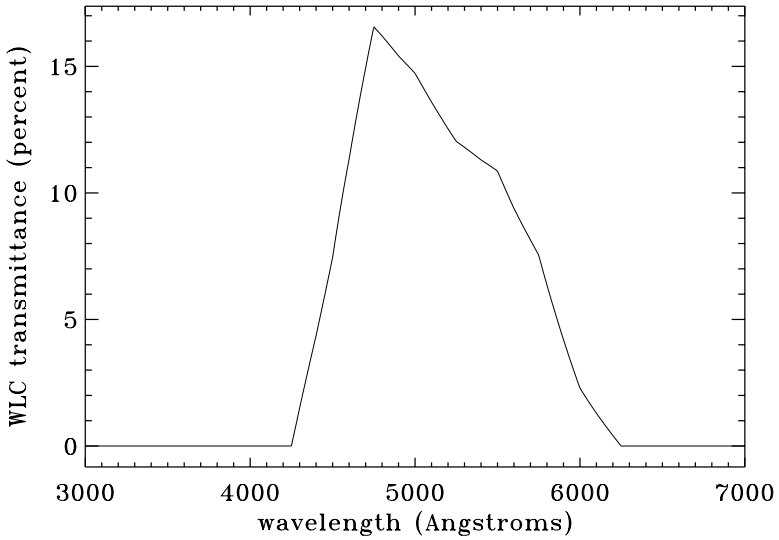

Figure 2: *WLC net bandpass transmittance, in percent.*

Finally, we wish to compute the ratio of the total (wavelength-integrated) intensity of Jupiter that makes it through the WLC bandpass to the analogous total Sun-center disk intensity. These two quantities are given by:

$$\langle I_{\rm J} \rangle \;=\; \int d\lambda \, I_{\lambda {\rm J}} \, T_1(\lambda) \, T_2(\lambda) \;\;=\;\; 3.9113 \times 10^{13} \text{ photons s}^{-1} \text{ cm}^{-2} \text{ sr}^{-1} \;, \tag{4}$$

$$\langle B_\odot \rangle \;=\; \int d\lambda \, B_{\lambda \odot} \, T_1(\lambda) \, T_2(\lambda) \;\;=\;\; 1.1511 \times 10^{20} \text{ photons s}^{-1} \text{ cm}^{-2} \text{ sr}^{-1} \;, \tag{5}$$

The ratio of these two quantities is 3.3980×10^{-7}, and the uncertainty on this number is approximately 7.1%, which is the quadrature sum (square root of the sum of the squares) of the uncertainties in a_λ and $T_1 T_2$. Note that the ratio $\langle I_{\rm J} \rangle / \langle B_\odot \rangle$ does not depend on the precise values of the solar flux and the WLC bandpass transmittance, but only on their relative wavelength dependence.

The above intensity ratio can be converted into a predicted count rate using the current version of the calibration in the UVCS Data Analysis Software (DAS). In this code, the conversion between intensity (in units of the Sun-center disk brightness) and count rate is given by

$$C \;=\; 2 \, f_{\rm rad} \left(\frac{w_{\rm occ}}{10} \right) \frac{\langle I_{\rm J} \rangle}{\langle B_\odot \rangle} \tag{6}$$

where C is the count rate in counts per second, $f_{\rm rad}$ is the radiometric calibration factor currently given by 7.67486×10^{10} counts sec^{-1} cm^{-1}, and $w_{\rm occ}$ is the width of the telescope mirror exposed by the internal occulter, in mm. For the January 1997 observations of Jupiter, the occulter width was 38.3673 mm, and thus the expected count rate for Jupiter should be 2.0012×10^5 counts per second.

Because of instrumental effects, the exact observed count rate would not be expected to be equal to the disk-center value derived above. The telescope's intrinsic point spread function smears out the intensity from Jupiter's disk, and this intensity may also be intrinsically limb-darkened. We model the instrumental point spread function as the convolution of two functions: P_1, the optical transfer function of the telescope, given as a Gaussian with a full-width at half-maximum (FWHM) of 10 arc seconds (Fineschi, private communication), and P_2, the quantization arising from the finite pinhole, which is a simple box function with a width of 14 arc seconds. (Note that we idealize the problem in one dimension, but the actual point spread functions are two-dimensional.) Figures 3a and 3b show P_1 and P_2.

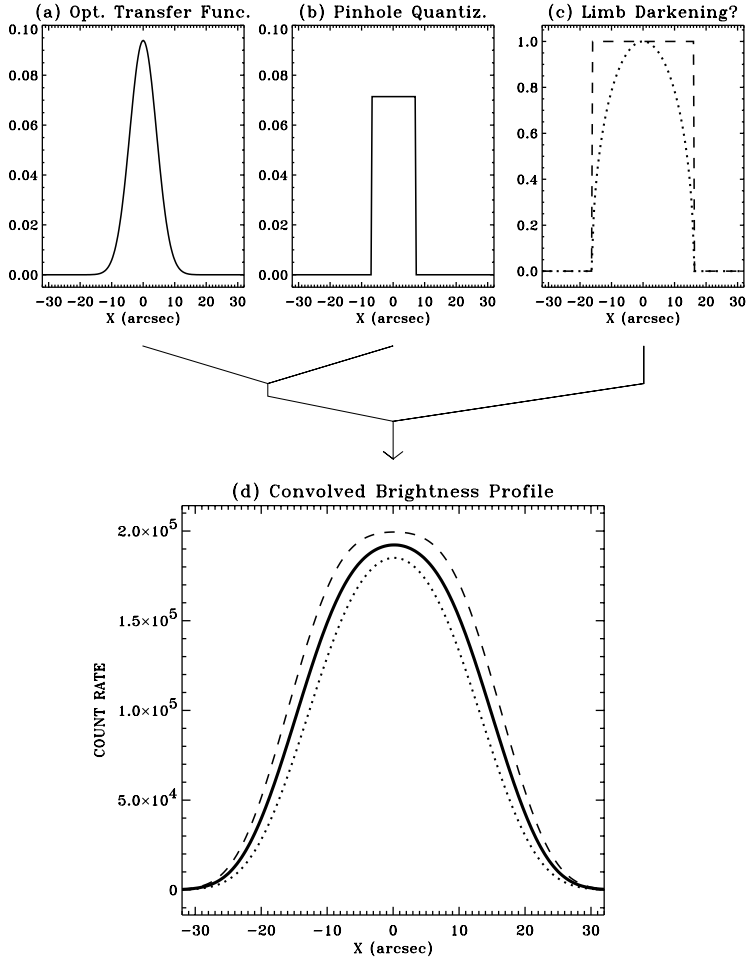

Figure 3: *Normalized point spread functions and sky-brightness distributions for Jupiter: (a) telescope optical transfer function P_1, (b) pinhole quantization P_2, (c) upper and lower limits on Jupiter's limb-darkening. The total convolution of all three functions is plotted in (d), in units of the expected count rate. (The thick solid line is an average between the upper and lower limit limb-darkening profiles.)*

Jupiter's intensity is observed to be limb-darkened strongly over its poles, but much less strongly over its equatorial cloud belts (see, e.g., Woodman et al. 1979). Thus, for the 1D (azimuthally averaged) intensity dependence we take reasonable upper and lower limits for the limb darkening. The upper limit is a flat, uniformly bright disk, and the lower limit is assumed to be linear limb darkening with the empirically derived

polar Minnaert constant K_d of 1 (Tejfel et al. 1994), or simply

$$I(r) \;=\; I(0)\sqrt{1-\frac{r^2}{R_{\rm J}^2}} \tag{7}$$

where r is the observed on-sky distance from the center of Jupiter, and $R_{\rm J}$ is its radius in the plane of the sky. Jupiter's mean radius is 71490 km, and for the January 1997 opposition its distance from the Earth was 6.1143 AU; this gives a sky radius $R_{\rm J}$ of 16.12 arc seconds. Figure 3c shows the upper and lower limits for the limb darkening, and Figure 3d shows the final convolution of the telescope point spread function (normalized to an integral of unity) with these intensity profiles (each normalized such that $I(0) = 2.0012 \times 10^5$ counts s^{-1}). The result looks approximately Gaussian, but with a flatter peak. The maximum in the expected count rates ranges between 1.85×10^5 and 1.99×10^5 counts s^{-1}. The spread arising from the uncertainty in the limb darkening is equivalent to an additional $\pm 3.6\%$ uncertainty in the peak count rate, which is summed in quadrature with the other uncertainties to give a net uncertainty of about $\pm 8\%$, for a predicted peak count rate of:

$$\max\,(C) \;\equiv\; (1.92 \pm 0.15) \times 10^5 \text{ counts s}^{-1} \;\;.$$

4. The Observations

Jupiter was observed for 3.66 hours with the WLC in January 1997, and in this time it moved across the sky by approximately 0.4 $R_\odot$. Thus, the UVCS commander had to track Jupiter's position and make pointing adjustments on an almost minute-by-minute basis. Figure 4 shows the commanded positions of the 123 exposures taken between 20:51 UT, 16 January and 00:31 UT, 17 January (there are often multiple exposures taken at the same positions).

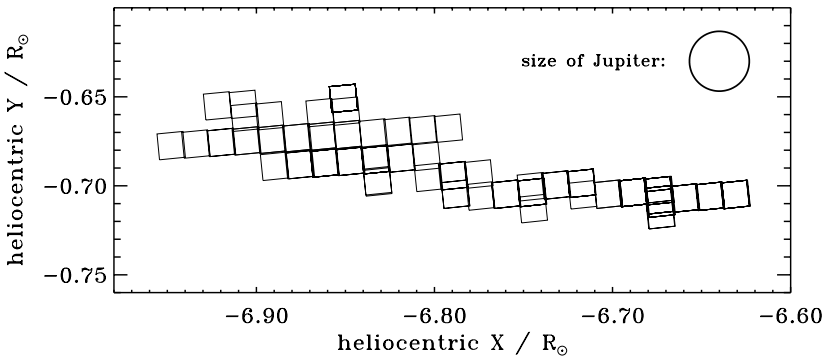

Figure 4: *January 1997 WLC observations of Jupiter's path, with the* $14'' \times 14''$ *WLC pixel positions and Jupiter's size on the sky both plotted to scale.*

In Figure 4, Jupiter moved from left to right over the 3.66 hours of the observation, and the WLC pixel followed it as closely as possible. For the first ∼1.1 hours, Jupiter was far from the pixel and the minimum count rate during this time was about 1200 counts s^{-1}. (This background contains contributions from instrumental scattering and the solar K and F coronae.) For the remainder of the observation, the count rate fluctuated rapidly between background values $< 10^4$ counts s^{-1} and periods of reasonably steady exposure at slightly greater than 10^5 counts s^{-1}. The maximum count rate observed, presumably when the pixel

was nearly centered on Jupiter, was 1.729×10^5 counts s^{-1}. Figure 5a shows the observed count rate as a function of time.

Data from the 1997 *Astronomical Almanac* allows us to derive a simple model of Jupiter's path across the sky, which is very nearly a straight line over a time period of a few hours. John Raymond's STARPOS code was used to translate right ascension and declination into Sun-centered Cartesian coordinates (with the observer translated from the Earth to the position of SOHO). Thus, the Cartesian coordinates of the center of the planet can be written as:

$$x_c(t) = x_{c0} + Vt \cos\theta \quad (8)$$
$$y_c(t) = y_{c0} + Vt \sin\theta \ . \quad (9)$$

where x_{c0} and y_{c0} denote the position of Jupiter's center at the start of the UVCS observation, V is its on-sky "velocity," t is the time measured from the start of the observation, in seconds, and θ is the angle between Jupiter's path vector and the west heliographic limb ($x > 0, y = 0$), measured counterclockwise. The data from the *Almanac* and the STARPOS code predict that $x_{c0} = -6.948\,R_\odot$, $y_{c0} = -0.6579\,R_\odot$, $V = 3.399 \times 10^{-5}\,R_\odot\ s^{-1}$, and $\theta = 353.8°$.

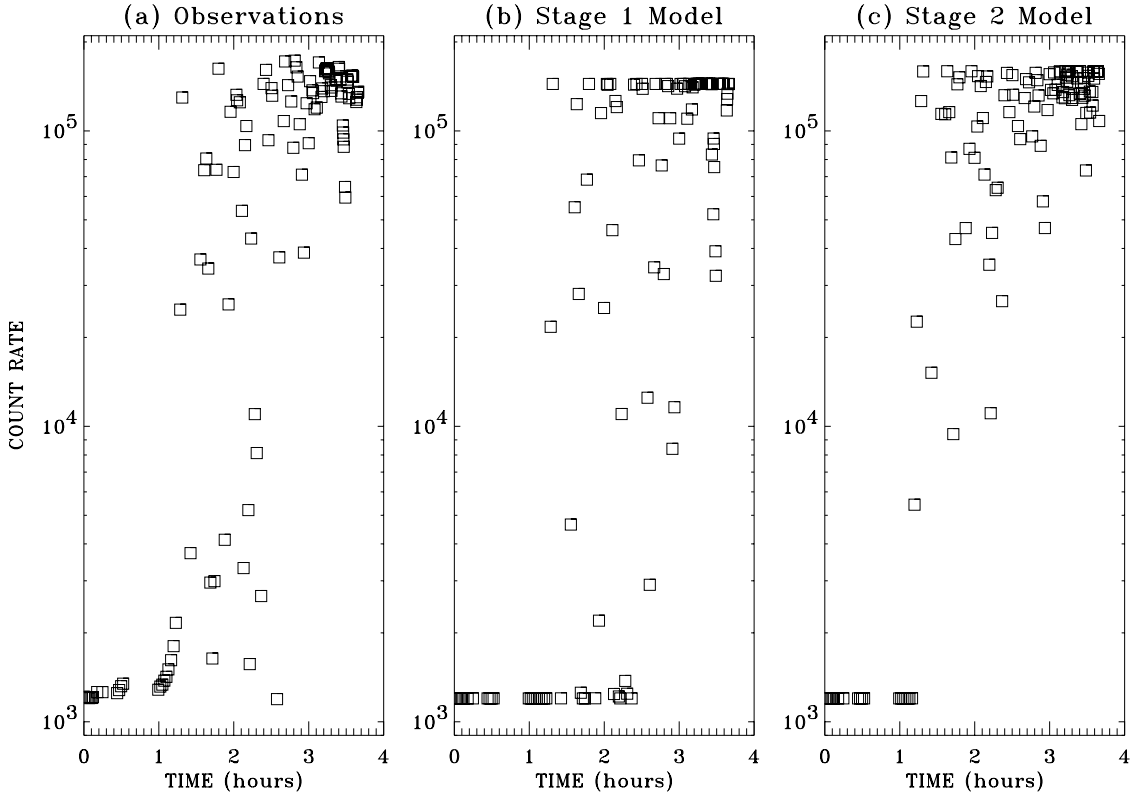

Figure 5: *Count rates as a function of time for: (a) the January 1997 observations, (b) the results of the simple χ^2 minimization in Stage 1, and (c) the results of the more involved parameter fitting in Stage 2.*

We are now in a position to compare the WLC data with the predictions of Jupiter's path and its count-rate profile (Figure 3d). It is fortuitous that the 123 exposures sampled a rather wide track in the sky, both on and off Jupiter. There are many exposures that point at the "shoulder" of the spread-out profile shown in

Figure 3d, as well at as its flattened peak. We thus have sufficient information to build an *"empirical model"* of both the path and the count-rate profile. The parameters of this model can then be varied until a best fit (with a minimum χ^2) is found with the data.

The expected count-rate profile $C(r)$ is given in Figure 3d, but for the empirical model we parameterize it as a flat-topped Gaussian function:

$$C(r) = \begin{cases} B_0 + C_0 & r < f \\ B_0 + C_0 \exp\left[-\left(\frac{r-f}{\sigma}\right)^2\right] & r \geq f \end{cases} \quad (10)$$

where B_0 is the background count rate when Jupiter is far from the aperture, C_0 is the maximum central count rate of Jupiter, f is the radius of the flat-topped portion of the profile, and σ is the $1/e$ half-width of the Gaussian portion of the profile.

Because of unexpected pointing uncertainties in the WLC data, the construction of the empirical model proceeded in two stages: (1) determination of Jupiter's path from the χ^2 minimization, and (2) determination of Jupiter's count-rate profile, along with the mean WLC pointing uncertainty, from the statistical properties of the data. The motivation behind this two-step process is explained below.

Stage 1. For the χ^2 minimization between the data and the model, there were 8 model parameters to vary: 4 for the path (x_{c0}, y_{c0}, V, θ) and 4 for the count-rate profile (B_0, C_0, f, σ). The standard nonlinear Levenberg-Marquardt algorithm for finding minima in χ^2 space was used, but because the parameter space was so topologically complex (8-dimensional!), a large ensemble of initial guesses was used to probe the space as completely as possible. More stable results were found if the parameter B_0 were fixed at a reasonable background value of 1200 counts s^{-1}, so for the final results of this stage only the other 7 parameters were varied.

A satisfactory minimum value of χ^2 was found, but the value of the *normalized* value of $\chi^2/(N-M)$, where N = 123 exposures and M = 7 parameters, was rather high: 1620. This value depends sensitively on the adopted uncertainties in the observed count rates. At this stage of the analysis, only Poisson statistics were included, which resulted in extremely small uncertainties for the large count rates ($\pm$ 0.3% at the lowest count rates, $\pm$ 0.05–0.1% at the highest count rates). Thus, the large χ^2 is understandable despite the high quality of the solution over a large dynamic range of count rates.

The path variables in this best solution were as follows: $x_{c0} = -7.097\,R_\odot$, $y_{c0} = -0.663\,R_\odot$, $V = 3.51 \times 10^{-5}\,R_\odot\ s^{-1}$, and $\theta = 354.2°$. The differences between these values and the predictions above are all less than 4%, and the values of y_{c0} and θ are within 1% of the predictions. The initial heliocentric radius of Jupiter is 0.149 $R_\odot$ larger than predicted above, which is a small relative difference, but important for absolute pointing. These differences may be related to the slow "drift" that has been observed to occur over $\sim$1 hour time scales when the mirror/occulter positions are changed.

The count-rate profile variables in this best solution were: B_0 = 1200 counts s^{-1}, $C_0 = 1.43 \times 10^5$ counts s^{-1}, f = 7.20 arc seconds, and σ = 6.05 arc seconds. An empirical model with these values reproduces the observed count rates reasonably well, but some detailed variations are not reproduced (compare Figures 5a and 5b). For count rates larger than 10^5 counts s^{-1}, the mean count rate is adequately modeled, but the spread of values about this mean is not modeled well. The observed standard deviation about the mean "high" count rate (i.e., excluding points with $C < 10^5$) is approximately 12% of the mean, which is much larger than both the spread in the model results and the expected Poisson uncertainties. *It is clear that some other source of count-rate variability must be included in order to understand the observations.*

Stage 2. In order to model realistically the instrumental response, we now introduce an effective "jitter" between the commanded pixel position and the actual, observed pixel position. For each observation, we assume this jitter is random in direction and has a random magnitude between 0 and a maximum radius

ξ. For observations of an isolated bright source such as Jupiter, this jitter can produce a large standard deviation in the observed count rate when near the planet, but effectively no additional standard deviation when observing the homogeneous background.

Thus, assuming the path variables and B_0 have been well-determined in Stage 1, we vary the four parameters C_0, f, σ, and ξ, with the goal of minimizing two quantities for the subset of observations with count rates greater than 10^5 counts s^{-1}:

- $\langle C \rangle$, the *mean* count rate (observed: 1.426×10^5 counts s^{-1})
- S, the *standard deviation* about the mean (observed: 1.717×10^4 counts s^{-1}).

The scalar quantity that is minimized is the product of χ^2 and an *ad hoc* "figure of merit" function $\mathcal{M}^2$ that indicates how close a given model is to the above two statistical quantities:

$$\mathcal{M}^2 \;=\; \left(\frac{\langle C \rangle_{\rm obs} - \langle C \rangle_{\rm model}}{\langle C \rangle_{\rm obs}} \right)^2 + \left(\frac{S_{\rm obs} - S_{\rm model}}{S_{\rm obs}} \right)^2 \quad . \tag{11}$$

The values of the parameters with the lowest resulting values of the product $\chi^2 \mathcal{M}^2$ are as follows: $C_0 = 1.58 \times 10^5$ counts s^{-1}, f = 3.05 arc seconds, σ = 22.43 arc seconds, and ξ = 11.71 arc seconds. The modeled count rates are plotted in Figure 5c. Note that C_0 is larger than the mean observed value of $\langle C \rangle$ because random jitter tends more often to move away from an isolated source than towards it. However, the modeled peak count rate ($C_0 + B_0$) is 17% smaller than the predicted peak value of 1.92×10^5 counts s^{-1} (see §3, above). This difference is smaller than the $\pm$25% systematic uncertainty that is commonly used in UVCS/WLC data analysis, but is probably significant, since it is greater than the $\pm$8% uncertainty in the predicted peak count rate.

Thus, if this result is to be trusted (and it should **not** be until it is independently verified), it would recommend that the WLC radiometric calibration factor of $f_{\rm rad} = 7.67486 \times 10^{10}$ counts sec^{-1} cm^{-1} should be revised *downward* to a value of about 6.36×10^{10} counts sec^{-1} cm^{-1}. This has the adverse effect of *increasing* predicted coronal intensities and polarized brightnesses, but only by 17% (well within the 25% [or even 50%] error bars used in the analysis of WLC data).

The values of f and σ are close to what was expected (compare with Figure 3d), and the value of ξ is small enough ($\sim$0.01 $R_\odot$) not to worry significantly about jitter from observation to observation when viewing the corona.

5. Postscript: June 2001

I am indebted to Rich Frazin for pointing out several errors in the above document that deserve mention. Taken together, the above result of good agreement between the UVCS laboratory calibration and the January 1997 Jupiter observation does not seem to hold up.

1. The right-hand side of equation (6) should contain an additional factor of 1/2, to account for the Müller matrix for unpolarized light. In other words, the actual I Stokes parameter is twice the measured intensity at any one of the three standard polarization angles. This factor of 1/2 cancels with the factor of 2 already on the right-hand side, and thus the value of C derived from equation (6) should be half as large as derived above.

2. There is no guarantee that the WLC was pointed accurately enough so that Jupiter filled the pixel completely. (This was done much better in the 2001 observation.) The maximum count rate observed in January 1997 was around 1.7×10^5 counts per second, but this is only a *lower limit* if the pixel was not fully centered on Jupiter.

3. The WLC occulter width was 38.4 mm, but the instrument is vignetted for exposed mirror areas in excess of about 35 mm. Thus there was less light on the mirror than was assumed in equation (6). This 9% effect is minor, but probably not negligible.

4. The conversion from incident solar flux to intensity reflected by Jupiter in equation (3) assumes that Jupiter acts as a gray atmosphere, like the Sun. Actually, it would be safer just to use a *geometrical* conversion factor between flux and intensity ($i.e., 1/\pi$) rather than the stated factor of ($5/4\pi$). This means that the dimensionless ratio $\langle I_{\rm J} \rangle / \langle B_\odot \rangle$ should be approximately 2.72×10^{-7}.

The end result of the above analysis (if correct!) implies that the correct value for C in equation (6) should have been only 7.3×10^4 counts per second. Taking account of the broadening functions depicted in Figure 3 reduces this, by about 4%, to 7.0×10^4 counts per second. Since the *observed* count rate of Jupiter was at least 1.7×10^5, this implies that the WLC radiometric calibration factor $f_{\rm rad}$ should be increased by a factor of (at least) 2.43 to a value of 1.86×10^{11} counts sec^{-1} cm^{-1}. This has the effect of *decreasing* actual coronal intensities by at least a factor of 2.43 (if Jupiter filled the pixel in 1997) or by *more* than a factor of 2.43 (if Jupiter did not fill the pixel in 1997).

REFERENCES

Altschuler, M. D., & Perry, R. M. 1972, Sol. Phys., 23, 410

Chandrasekhar, S. 1960, Radiative Transfer (New York: Dover)

Drossart, P., & Encrenaz, T. 1983, Icarus, 55, 390

Harris, D. L. 1961, "Photometry and Colorimetry of Planets and Satellites," in Planets and Satellites, ch. 8, vol. III of The Solar System, ed. G. P. Kuiper and B. M. Middlehurst (U. Chicago Press), 272

Kohl, J. L., et al. 1995, Sol. Phys., 162, 313

Kurucz, R. L., Furenlid, I., Brault, J., & Testerman, L. 1984, Solar Flux Atlas from 296 to 1300 nm, (Sunspot, NM: National Solar Observatory), data on the World Wide Web at: `http://cfaku5.harvard.edu/`

Minnaert, M. 1930, ZAp, 1, 209

Munro, R. H., & Jackson, B. V. 1977, ApJ, 213, 874

Romoli, M., Weiser, H., Gardner, L. D., & Kohl, J. L. 1993, Applied Optics, 32, 3559

Rybicki, G. B., & Lightman, A. P. 1979, Radiative Processes in Astrophysics (New York: John Wiley and Sons)

Tejfel, V. G., Vdovichenko, V. D., Sinyaeva, N. V., Mosina, S. A., Gajsina, W. N., Kharitonova, G. A., & Aksenov, A. N. 1994, J. Geophys. Res., 99, 8411

van de Hulst, H. C. 1950, Bull. Astron. Inst. Netherlands, 11, 135

Woodman, J. H., Cochran, W. D., & Slavsky, D. B. 1979, Icarus, 37, 73

This preprint was prepared with the AAS LaTeX macros v4.0.